Nonlinear wind wave model under wind forcing and dissipation

Wenhao Cheng, Zeng Liu*
School of Naval Architecture and Ocean Engineering, Huazhong University of Science and Technology, Wuhan, Hubei, China
z_liu@hust.edu.cn

1 INTRODUCTION

In 1847, Stokes[1] gave the existence of two-dimensional uniform propagating solutions, known as Stokes waves. Later, Benjamin[2] demonstrated that wave trains in deep water are unstable to modulational perturbations, such a phenomenon is called "Benjamin-Feir"(BF) instability or modulational instability.

Early studies about BF instability primarily neglected effects of dissipation and wind forcing. Segur[3] proved that dissipation can stabilize the instability based on a damped version of the nonlinear Schrödinger equation. This stabilization theory was validated by Ma[4] through experiments. Kharif[5] showed that the wind speed strength influences modulational instability and these results were validated by Touboul[6] using potential equations.

In this work, the fully nonlinear wave evolution equations are numerically solved, and the long-time evolution of modulational instability wave trains under wind forcing and dissipation effects is analyzed.

2 MATHEMATICAL FORMULATION

We consider the evolution of a two-dimensional gravity water waves with a free surface in deep water under the effect of wind forcing and dissipation. The fluid is assumed to be irrotational, inviscid and incompressible. Let z denotes the vertical coordinate, x the horizontal coordinate, t the time, $z = \eta(x,t)$ the free surface and $\Phi(x,z,t)$ the velocity potential, respectively. The governing equation for the water waves is

$$\frac{\partial^2 \Phi}{\partial x^2} + \frac{\partial^2 \Phi}{\partial z^2} = 0, \quad -h < z < \eta(x,t), \tag{1a}$$

$$\frac{\partial \Phi}{\partial z} = 0, \quad z = -h, \tag{1b}$$

$$\frac{\partial \eta}{\partial t} = \left(1 + \left(\frac{\partial \eta}{\partial x}\right)^2\right) \frac{\partial \Phi_s}{\partial z} - \frac{\partial \eta}{\partial x}\frac{\partial \Phi_s}{\partial x} + 2\nu \frac{\partial^2 \eta}{\partial x^2}, \tag{1c}$$

$$\frac{\partial \Phi_s}{\partial t} = -g\eta - \frac{1}{2}\left(\frac{\partial \Phi_s}{\partial x}\right)^2 + 2\nu \frac{\partial^2 \Phi_s}{\partial x^2} + \frac{1}{2}\left(1 + \left(\frac{\partial \eta}{\partial x}\right)^2\right)\left(\frac{\partial \Phi_s}{\partial z}\right)^2 - \frac{P_{wind}}{\rho_w}, \tag{1d}$$

where $\Phi_s = \Phi|_{z=\eta}$ is the vertical velocity of the fluid at the free surface, g is the gravitational acceleration, h is the water depth, P_{wind} is the pressure of wind forcing and ν, ρ_w is the eddy viscosity and density of water, respectively. The numerical method used to solve Eqs. (1) in this study is the Pseudospectral Fourier-Legendre method (PFL method) proposed by [7].

3 NUMERICAL RESULTS

In this work, we simulate the modulational Stokes wavetrain due to type I instabilities under no wind action and five different wind speed conditions(1.4, 2.3, 3.2, 4.1, 5.0 m/s). The initial condition is the same as [8]:

$$\eta(x,0) = \eta_0[0.13,9] + 0.1a_0\cos\left(7x - \frac{1}{4}\pi\right) + 0.1a_0\cos\left(11x - \frac{1}{4}\pi\right), \tag{2a}$$

$$\Phi^s(x,0) = \Phi_0^s[0.13,9] + 0.1a_0\sqrt{\frac{g}{7}}\sin\left(7x - \frac{1}{4}\pi\right) + 0.1a_0\sqrt{\frac{g}{11}}\sin\left(11x - \frac{1}{4}\pi\right), \tag{2b}$$

where $\eta_0[0.13,9]$ is the fifth-order Stokes wave, 0.13 is wave steepness, 9 is the fundamental wavenumber, and $a_0 = 0.13/9$ is the initial amplitude of the fundamental wave.

Fig.1 presents spatial profiles of the free-surface elevation $z = \eta$ at different times under no wind action and wind speed of $4.1m/s$. Compared to no wind forcing condition, the wave height and the dominant wavenumber decrease remarkably under the wind forcing.

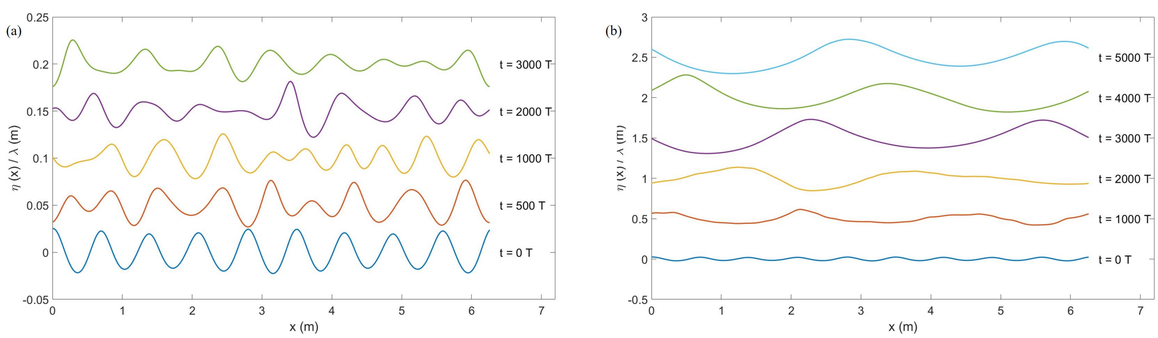

Figure 1: Variations of spatial profiles of free surface $z = \eta$ with time under (a) no wind action and (b) wind speed of $4.1m/s$.

Fig.2 shows the time histories of amplitudes of wave components during evolution under no wind action and wind speed of $4.1m/s$. Under no wind action, the evolution can be simply divided into the modulational stage (from 0 T to 800 T) and the nonlinear interaction stage (from 800T to 3000T). Under wind forcing condition, the dominant wavenumber of the wave trains transitions from $k = 9$ to $k = 2$. The amplitude of the largest wave component $k = 2$ increases to its maximum at $t \approx 3200\ T$, and then remains almost constant with time.

Variations of the dominant wavenumber of the wave trains during the evolution under different wind conditions are shown in fig.3. Under no wind action, the dominant wavenumber decreases from $k = 9$ to $k = 7$. Under wind forcing conditions, the dominant wavenumber of the wave trains decreases from $k = 9$ to $k = 2$, and increasing wind speed can accelerate this process.

The total wave energy E is calculated as $E = \int_{S_0} \Phi_s \eta_t dx + \int_{S_0} \eta^2 dx$, where S_0 is the horizontal plane. Time histories of total energy during evolutions under different wind conditions are shown in fig.4. Under no wind action, the wave energy continues to decrease and the wave trains break twice during this process. Under wind forcing conditions, the total

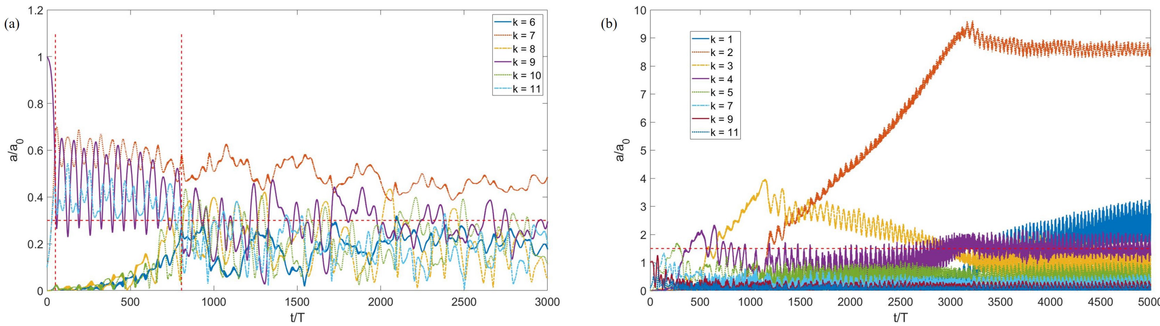

Figure 2: Variations of wave amplitude of different wave components with time under (a) no wind action and (b) wind speed of $4.1m/s$. The vertical dashed lines refer to the time when the wave breaking happened. Wave components below the horizontal dashed line during the evolution process are hidden for clarity except for the initial wave components.

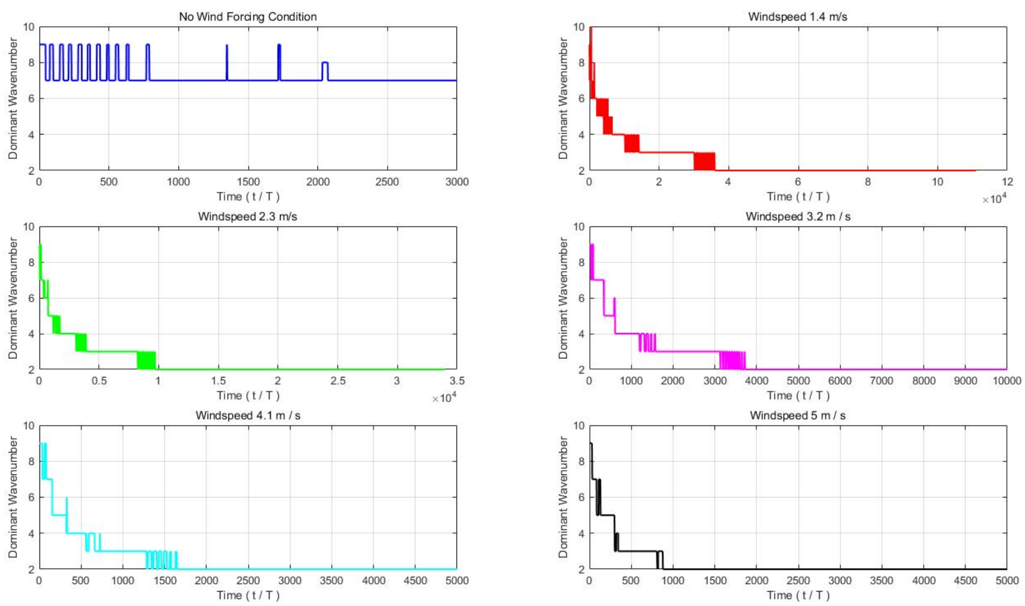

Figure 3: Variations of the dominant wavenumber during the evolution under different wind forcing conditions.

wave energy grows continuously and then reaches a balanced state with periodic changes, which means that the energy input by the wind balances the energy dissipation.

4 CONCLUTION

The evolutions of modulational instability wave trains with and without wind forcing are obtained and studied. Time histories of the free-surface spatial profiles, different wave component amplitudes, dominant wavenumber, and total wave energy are investigated. For wave groups under no wind action, the wave trains break twice, the dominant wave number decreases slightly and the wave energy decreases continuously. Under the wind forcing condi-

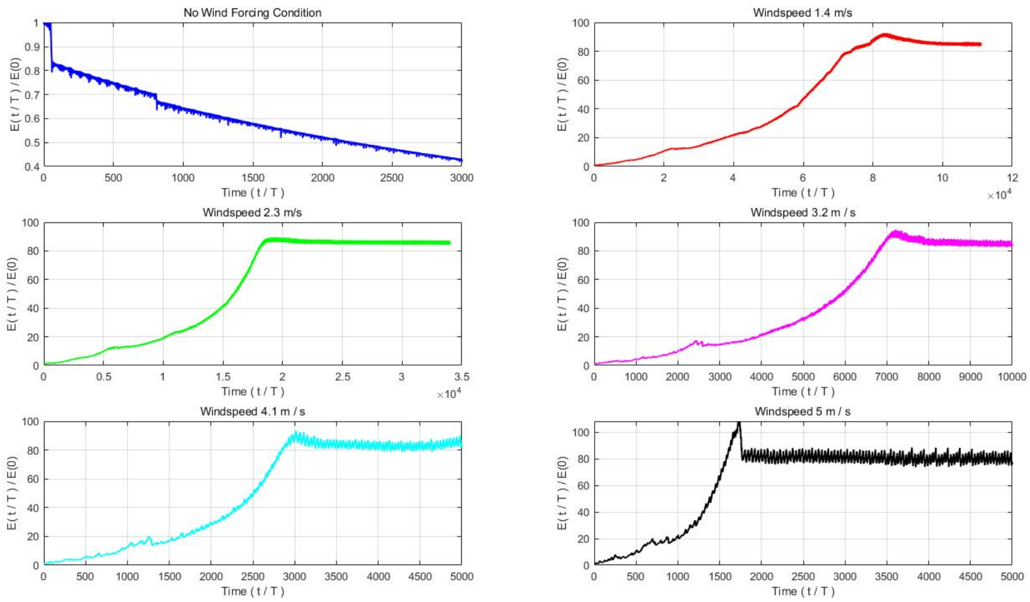

Figure 4: Variations of total wave enregy with time under different wind forcing conditions.

tions, the wave trains break frequently and the dominant wavelength increases remarkablely. The total wave energy increases first and then reaches a balanced state. The present study provides an analysis of the impact of wind on water wave evolution and these findings can help better understand wind wave behaviour.

REFERENCES

[1] Stokes, G. G. 1847. *On the theory of oscillatory waves. Trans. Cambridge Phil. Soc. 8*, 411–455.

[2] Benjamin, T. B., and Feir, J. E. 1967. *The disintegration of wave trains on deep water. Part 1. Theory. J. Fluid Mech. 27(3)*, 417–430.

[3] Segur, H., Henderson, D., Carter, J., Hammack, J., Li, C.-M., Pheiff, D., and Socha, K. 2005. *Stabilizing the benjamin-feir instability. J. Fluid Mech. 539*, 229–271.

[4] Ma, Y., Dong, G., Perlin, M., Ma, X., and Wang, G. 2012. *Experimental investigation on the evolution of the modulation instability with dissipation. J. Fluid Mech. 711*, 101–121.

[5] Kharif, C., Kraenkel, R. A., Manna, M., and Thomas, R. 2010. *The modulational instability in deep water under the action of wind and dissipation. J. Fluid Mech. 664*, 138–149.

[6] Touboul, J., and Kharif, C. 2010. *Nonlinear evolution of the modulational instability under weak forcing and damping. Nat. Hazard. Earth Sys. 10*, 2589–2597.

[7] Klahn, M., Madsen, P. A., and Fuhrman, D. R. 2021. *Simulation of three-dimensional nonlinear water waves using a pseudospectral volumetric method with an artificial boundary condition. Int. J. Numer. Meth. Fluids 93(6)*, 1843–1870.

[8] Dommermuth, D. G., and Yue, D. K. 1987. *A high-order spectral method for the study of nonlineaer gravity waves. J. Fluid Mech. 184*, 267–288.